Available online at www.sciencedirect.com

SciVerse ScienceDirect

Ceramics International 38 (2012) 5941–5947

CERAMICS INTERNATIONAL

www.elsevier.com/locate/ceramint

$SrCo_{1-x}Sb_xO_{3-\delta}$ cathode materials prepared by Pechini method for solid oxide fuel cell applications

Sea-Fue Wang *, Hsi-Chuan Lu, Yung-Fu Hsu, Chien-Chung Huang, Chun-Ting Yeh

Department of Materials and Mineral Resources Engineering, National Taipei University of Technology, Taipei 106, Taiwan, ROC

Received 2 February 2012; received in revised form 1 April 2012; accepted 14 April 2012
Available online 20 April 2012

Abstract

In this study, $SrCo_{1-y}Sb_yO_{3-\delta}$ powders were prepared by a modified Pechini method. According to the study results, the cubic Pm3m phase of the $SrCo_{1-y}Sb_yO_{3-\delta}$ ceramics was obtained as 10% of cobalt ions were substituted by antimony ions. Doping of Sb^{3+} ions appeared both to stabilize the Pm3m phase of the $SrCo_{1-y}Sb_yO_{3-\delta}$ ceramics and to enhance densification and retard grain growth. The coefficient of thermal expansion of the $SrCo_{1-x}Sb_xO_{3-\delta}$ ceramics increased with the content of the antimony ions, ranging from 10.17 to 15.37 ppm/°C at temperatures lower than the inflection point (ranging from 450 °C to 550 °C) and from 22.16 to 29.29 ppm/°C at higher temperatures. For the $SrCo_{0.98}Sb_{0.02}O_{3-\delta}$ ceramic, electrical conductivity reached a maximum of 507 S/cm at 450 °C. The ohmic and polarization resistances of the single cell with the pure $SrCo_{0.98}Sb_{0.02}O_{3-\delta}$ cathode at 700 °C read respectively 0.298 Ω cm^2 and 0.560 Ω cm^2. The single cell with the $SrCo_{0.98}Sb_{0.02}O_{3-\delta}$-SDC composite cathode appeared to reduce the impedances with the R_0 and R_P at 700 °C reading respectively 0.109 Ω cm^2 and 0.127 Ω cm^2. Without microstructure optimization and measured at 700 °C, the single cells with the pure $SrCo_{0.98}Sb_{0.02}O_{3-\delta}$ cathode and the $SrCo_{0.98}Sb_{0.02}O_{3-\delta}$-SDC composite cathode, demonstrated maximum power densities of 0.100 W/cm^2 and 0.487 W/cm^2. Apparently, $SrCo_{1-y}Sb_yO_{3-\delta}$ is a potential cathode for use in IT-SOFCs.

Keywords: Solid oxide fuel cell; Cathode; Impedance; Cell performance

1. Introduction

Solid oxide fuel cell (SOFC) system is considered to have superior potential for commercialization due to its high energy conversion efficiency, self-reforming ability, compatibility with common hydrocarbon fuels, use of solid state materials, and no need for noble metal catalysts [1,2]. SOFC can be used in large-size stationary power facilities or applied to heat and power generation for homes and businesses as well as auxiliary power units for electrical systems in transportation vehicles. In recent years, enormous research efforts have been invested on the development of intermediate temperature SOFCs (IT-SOFCs) capable of operating at temperatures between 500 and 700 °C [3]. The performance of IT-SOFCs depends strongly on the ionic conductivity of electrolyte and the polarization resistance (R_P) of electrodes [4]. The former feature can be enhanced by using alternative electrolytes with a higher ionic conductivity at low temperatures, such as $La_{0.9}Sr_{0.1}Ga_{0.8}Mg_{0.2}O_{3-\delta}$ (LSGM) and $Sm_{0.2}Ce_{0.8}O_{2-\delta}$ (SDC), or by using a thin yttria-stabilized zirconia (YSZ) electrolyte film [5]. The latter feature is usually improved by tailoring electrode configurations or by utilizing new electrode materials. Since oxygen reduction reaction is generally thought to be more difficult to activate on SOFCs operating at intermediate temperatures, the cathode is often the limiting resistance of the SOFC cell because of its large overpotential [6].

Though a preferred cathode material for use with YSZ at high temperatures (>850 °C), $La_{1-x}Sr_xMnO_3$ (LSM) tends to perform poorer at temperatures below 800 °C [6,7]. The performance of LSM cathode declines drastically as the operating temperature drops, due to its low oxygen ion conductivity and high activation energy for oxygen disassociation [6,8]. Alternative cathodes are thus needed for SOFCs to operate at lower temperatures. Researchers have accordingly proposed the strategy of utilizing materials with mixed ionic/electronic conductivity (MIEC) [9,10]. MIEC materials help extend the three-phase boundary (TPB) of the electrolyte (ionic

* Corresponding author. Present address: Department of Materials and Mineral Resources Engineering, National Taipei University of Technology, 1, Sec. 3, Chung-Hsiao E. Rd., Taipei 106, Taiwan, ROC.
Tel.: +886 2 2771 2171x2735; fax: +886 2 2731 7185.
E-mail address: sfwang@ntut.edu.tw (S.-F. Wang).

0272-8842/$36.00
http://dx.doi.org/10.1016/j.ceramint.2012.04.046

conductor), cathode (electronic conductor) and gas (oxygen or air used as an oxidant) phases to the entire cathode–gas interface, thereby resulting in dramatic improvement of the cathode's electrochemical performance [8,11].

Perovskite oxide $SrCoO_{3-\delta}$ is a very important parent compound essential for the development of various functional materials like oxygen separation membranes, methane conversion reactors, and SOFC cathodes [12–18]. $SrCoO_{3-\delta}$ oxide exists in three different polymorphs, including the oxygen vacancy-ordered orthorhombic brownmillerite phase below 653 °C, the 2-H type hexagonal phase between 653 and 920 °C, and the cubic perovskite phase above 920 °C. Of the three polymorphs, the cubic-structured, high-temperature $SrCoO_{3-\delta}$ is capable of serving as a MIEC material exhibiting the highest electrical conductivity and oxygen permeability. Therefore doped cations for either A-site or B-site of $SrCoO_{3-\delta}$ are commonly used to stabilize the high-temperature cubic phase at lower temperatures. Doped $SrCoO_{3-\delta}$ perovskite oxides, such as $SrCo_{1-y}Nb_yO_{3-\delta}$ [12,13], $SrCo_{1-y}Sb_yO_{3-\delta}$ [15,16], and $SrCo_{1-y}Sc_yO_{3-\delta}$ [14], have been used as potential cathode materials for IT-SOFCs. In this study, $SrCo_{1-y}Sb_yO_{3-\delta}$ (SCS; $y = 0.00–0.20$) oxides were prepared via a modified Pechini method. The structural, electrical, and electrochemical properties of the prepared $SrCo_{1-y}Sb_yO_{3-\delta}$ oxides as potential cathode materials were investigated and assessed. The performance of the single cell based on NiO–SDC/$Sm_{0.2}Ce_{0.8}O_{2-\delta}$ (SDC)/$SrCo_{1-y}Sb_yO_{3-\delta}$ was also evaluated.

2. Experimental procedure

The $SrCo_{1-y}Sb_yO_{3-\delta}$ powders were prepared by a modified Pechini method. Highly pure (>99.9% purity) Sb_2O_3 (STREM, Reagent grade), $Sr(NO_3)_2$ (ACROS, Reagent grade), $Co(NO_3)_2{\cdot}6H_2O$ (ACROS, Reagent grade), and citric acid (SHOWA, Reagent grade) were used as raw materials. Stoichiometric amounts of Sb_2O_3, $Sr(NO_3)_2$ and $Co(NO_3)_2{\cdot}6H_2O$ based on the composition of $SrCo_{1-y}Sb_yO_{3-\delta}$ ($y = 0.02$, 0.05, 0.10, and 0.15) were dissolved in a citric acid aqueous solution whose concentration was controlled at 0.3 M. The solution with metal ions and citric acid in the molar ratio of 1:1.2 was slowly stirred, heated at 70 °C for 6 h, and subsequently evaporated under IR irradiation, leaving eventually a black organic gel. Black $SrCo_{1-y}Sb_yO_{3-\delta}$ powders were then obtained after calcination at 900 °C for 12 h. The powders were milled in methyl alcohol solution, using polyethylene jars and zirconia balls for 24 h, to break down the agglomerates and then oven-dried at 80 °C for overnight. Phase identification on the calcined powders was performed using X-ray diffraction (XRD, Simens D5000). For electrical conductivity measurement, a 5 wt% of 15%-PVA solution was added to the powder which was in turn pressed into disc-shaped compacts under a uniaxial pressure of 0.9 tons/cm^2. The samples were then heat treated at 550 °C for 4 h to eliminate the PVA, followed by sintering at 1175 °C for 24 h (heating rate = 10 °C/min). Densities of the specimens were measured using the liquid displacement method. SEM (scanning electron microscopy, Hitachi S4700) studies on the polished and thermally etched surfaces of the sintered cells were conducted to examine cross-sectional microstructures. Conductivity as a function of temperature was measured by a standard four-probe method in air using Keithley 2400 at temperatures ranging from 25 °C to 800 °C. Coefficient of thermal expansion was determined from the dilatometer curve of the dense samples (NETZSCH 402 C) at a heating rate of 5 °C/min.

Commercially available raw materials for SOFC, including $Sm_{0.2}Ce_{0.8}O_{2-\delta}$ (SDC; Fuel Cell Materials, USA; $d_{50} = 0.53$ μm and BET surface area = 6.2 m^2 g^{-1}) and NiO (anode functional layer: Fuel Cell Materials, USA; current collector layer: SHOWA, Japan), were used in this study. Two kinds of NiO powders were utilized to build the SOFCs. One with a smaller particle size ($d_{50} = 0.8$ μm and BET surface area = 3.4 m^2 g^{-1}) was used for the anode functional layers, and the other with a larger particle size ($d_{50} = 10.1$ μm and BET surface area = 0.06 - m^2 g^{-1}) for the anode current collector layer. The anode-supported substrates incorporate a SDC electrolyte layer and a three-layer anode composed of a current collector layer (outer layer) of pure NiO and two functional layers of NiO–SDC composites with ratios of 60 wt%/40 wt% and 50 wt%/50 wt% respectively. Built via a tape casting process, the anode-supported substrates with a size of 25 mm in diameter and 0.5 mm in thickness were co-fired at 1400 °C for 2 h at a heating rate of 2 °C/min. Two kinds of cathodes, one with pure $SrCo_{1-y}Sb_yO_{3-\delta}$ powders and the other with $SrCo_{1-y}Sb_yO_{3-\delta}$-SDC composite (60 wt%/40 wt%), were prepared by screen-printing cathode pastes on the anode-supported SDC substrates. The cathodes were then fired at 1000 °C for 2 h. The electrochemical performance of the single cells was measured at the set-up of a commercially available ProboStat (NorECs, Norway). Detailed procedures of the electrochemical test were described in a previous paper [19].

3. Results and discussion

Fig. 1 shows the XRD patterns of the $SrCo_{1-y}Sb_yO_{3-\delta}$ ceramics calcined at 900 °C and subsequently sintered at

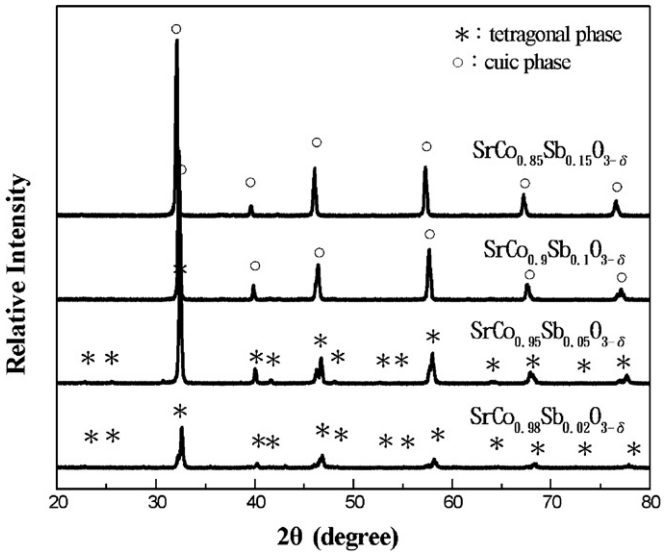

Fig. 1. XRD patterns of $SrCo_{1-x}Sb_xO_{3-\delta}$ ceramics sintered at 1175 °C for 24 h.

Table 1
Densities of $SrCo_{1-x}Sb_xO_{3-\delta}$ ceramics sintered at 1175 °C for 24 h.

Composition	Sintered density (g/cm^3)	Theoretical density (g/cm^3)	% Theoretical density (g/cm^3)
$SrCo_{0.98}Sb_{0.02}O_{3-\delta}$	4.78 ± 0.14	5.43	88.03%
$SrCo_{0.95}Sb_{0.05}O_{3-\delta}$	4.94 ± 0.25	5.48	90.15%
$SrCo_{0.9}Sb_{0.1}O_{3-\delta}$	5.31 ± 0.33	5.57	95.33%
$SrCo_{0.85}Sb_{0.15}O_{3-\delta}$	5.64 ± 0.07	5.66	99.65%

1175 °C for 24 h. As indicated, the $SrCo_{1-y}Sb_yO_{3-\delta}$ ceramics with $x = 0.02$ and 0.05 ($SrCo_{0.98}Sb_{0.02}O_{3-\delta}$ and $SrCo_{0.95}Sb_{0.05}O_{3-\delta}$) reported a tetragonal structure while the ceramics with $y > 0.10$ (including the $SrCo_{0.9}Sb_{0.1}O_{3-\delta}$ and $SrCo_{0.85}Sb_{0.15}O_{3-\delta}$ ceramics) appeared to exhibit a cubic structure. As observed by Aguadero et al. [15], a phase transition of the $SrCo_{1-y}Sb_yO_{3-\delta}$ ceramics, synthesized via the nitrate–citrate route, took place as the y value reached 0.20. In our study, the $SrCo_{1-y}Sb_yO_{3-\delta}$ powders were prepared by a modified Pechini method characterized by high purity, better chemical homogeneity, and good compositional control. It was found that the cubic Pm3m phase of the $SrCo_{1-y}Sb_yO_{3-\delta}$ ceramics was stabilized as 10% of the cobalt ions were substituted by antimony ions. It is thus apparent that the preparation method has a considerable effect on the phase structure of the doped oxides, as reported in the literature [14].

Table 1 lists the densities of the $SrCo_{1-x}Sb_xO_{3-\delta}$ ceramics sintered at 1175 °C for 24 h. Theoretical densities of the ceramics were calculated based on the lattice constants obtained from the XRD patterns, and densification was obviously enhanced with the doping of antimony ions in the cobalt-ion positions. The relative density of the sintered ceramics escalated from 88.03% to 99.65% as the y value increased from 0.02 ($SrCo_{0.98}Sb_{0.02}O_{3-\delta}$) to 0.15 ($SrCo_{0.85}Sb_{0.15}O_{3-\delta}$). This may be due to the fact that Sb_2O_3 reports a significantly lower melting point (656 °C) as compared to that of Co_2O_3 (1900 °C). As shown in Fig. 2, the corresponding SEM microstructures are in accord with the density data. Low densification (88.03% theoretical density) of the $SrCo_{0.98}Sb_{0.02}O_{3-\delta}$ ceramic led to a microstructure marked with a wide pore size distribution. The microstructure of the $SrCo_{0.95}Sb_{0.05}O_{3-\delta}$ ceramic reveals coalescence of pores associated with the sintering process. As the content of antimony ions continued to increase, densification underwent dramatic improvement, and a dense microstructure with isolated pores (1–3 μm) was observed. The $SrCo_{0.85}Sb_{0.15}O_{3-\delta}$ ceramics achieving the highest sintered density (99.65% theoretical density) demonstrated a microstructure with a dense and fine grain size. It appeared that the doping of antimony ions not only stabilized the Pm3m phase of the $SrCo_{1-y}Sb_yO_{3-\delta}$ ceramics but also sped up densification and slowed down grain growth.

Fig. 3 presents the dilatometrical results of the $SrCo_{1-x}Sb_xO_{3-\delta}$ ceramics sintered at 1175 °C for 24 h. The change in the slope of the dilatometric curves that occurred during the temperature range from 450 °C to 550 °C and led to

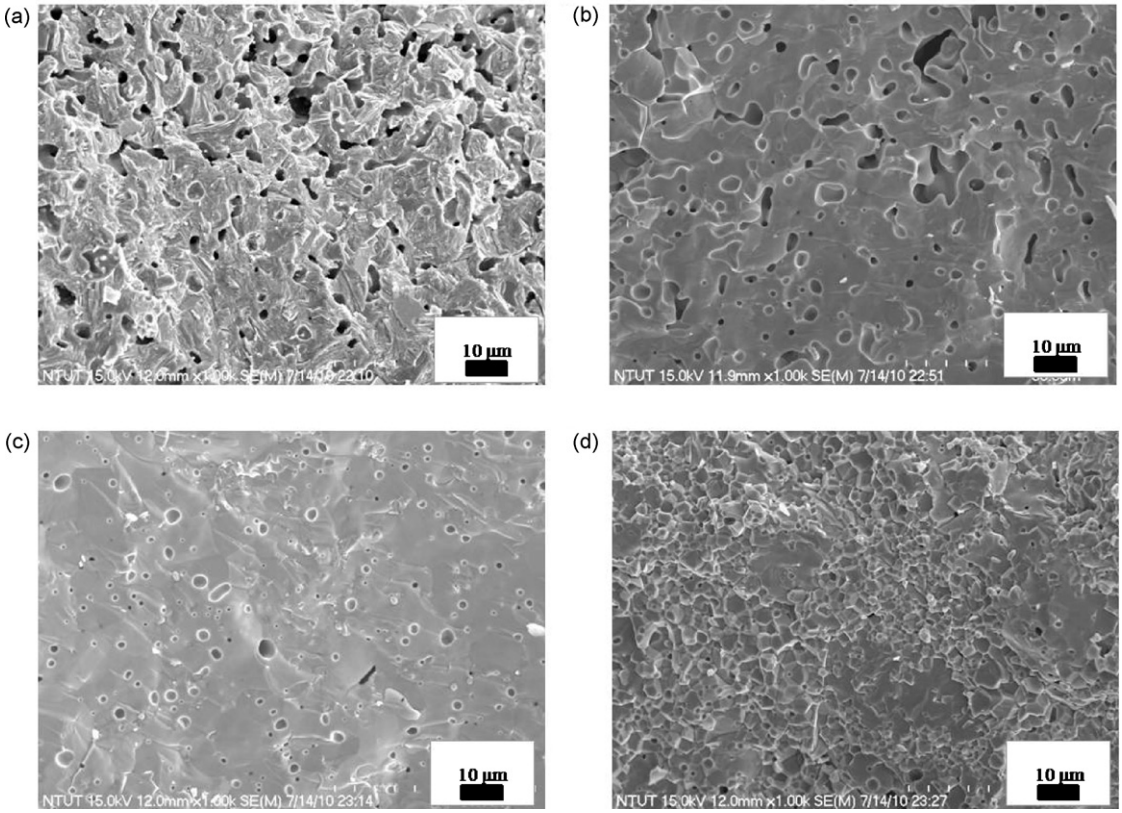

Fig. 2. SEM micrographs of fracture surfaces of (a) $SrCo_{0.98}Sb_{0.02}O_{3-\delta}$, (b) $SrCo_{0.95}Sb_{0.05}O_{3-\delta}$, (c) $SrCo_{0.9}Sb_{0.1}O_{3-\delta}$, and (d) $SrCo_{0.85}Sb_{0.15}O_{3-\delta}$ ceramics sintered at 1175 °C for 24 h.

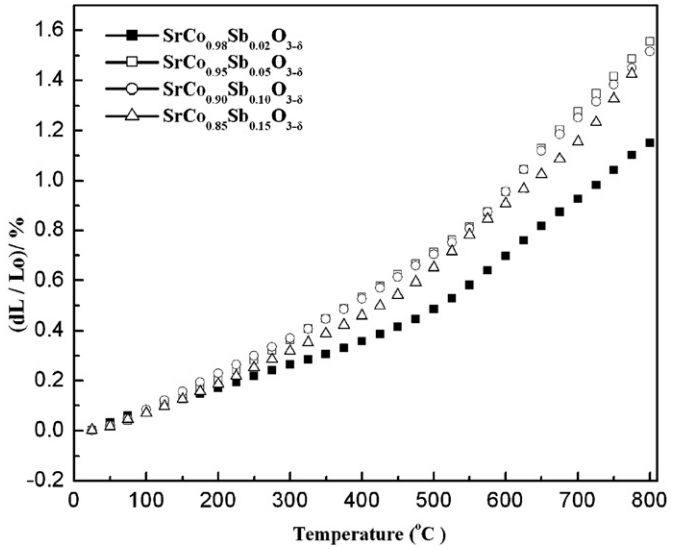

Fig. 3. Dilatometrical results of $SrCo_{1-x}Sb_xO_{3-\delta}$ ceramics sintered at 1175 °C for 24 h.

an inflection point was attributed to the beginning oxygen exchange of the materials [20–22]. A repulsion force arose between the mutually exposed cations when oxygen ions were extracted from the lattice, thus causing lattice expansion. An additional chemical expansion took place due to the reduction of the Co ions from higher to lower valences (ex. Co^{3+} ions were reduced to the larger Co^{2+} ions), occurring in conjunction with the creation of oxygen vacancies (increasing oxygen non-stoichiometry) to retain the electrical neutrality at high temperatures [23,24]. The corresponding coefficients of thermal expansion of the $SrCo_{1-x}Sb_xO_{3-\delta}$ ceramics below and above the inflection point are listed in Table 2. CTE in general increases with the content of the doped antimony ions, ranging from 10.17 to 15.37 ppm/°C at low temperatures and 22.16 to 29.29 ppm/°C at high temperatures. The CTEs of the $SrCo_{1-x}Sb_xO_{3-\delta}$ ceramics below the inflection point appeared to be very close to those reported by Aguadero et al. [15] while, with the exception of the $SrCo_{0.85}Sb_{0.15}O_{3-\delta}$ ceramic, the values above the inflection point emerged to be larger. The CTE values are equal to or larger than that of the commonly used $Sm_{0.2}Ce_{0.8}O_{2-\delta}$ cathode (SDC: 12.6 ppm/°C) [25,26]. A composite cathode made of cathode and electrolyte materials is generally employed to minimize the CTE mismatch at the electrolyte/cathode interface [27].

Illustrated in Fig. 4(a) are the electrical conductivities of the $SrCo_{0.98}Sb_{0.02}O_{3-\delta}$, $SrCo_{0.95}Sb_{0.05}O_{3-\delta}$, $SrCo_{0.9}Sb_{0.1}O_{3-\delta}$, and

Table 2
Coefficients of thermal expansion of $SrCo_{1-x}Sb_xO_{3-\delta}$ ceramics sintered at 1175 °C for 24 h.

Composition	Coefficients of thermal expansion (10^{-6} K^{-1})	
	R.T.~500 °C	500–800 °C
$SrCo_{0.98}Sb_{0.02}O_{3-\delta}$	10.17	22.16
$SrCo_{0.95}Sb_{0.05}O_{3-\delta}$	14.15	25.53
$SrCo_{0.90}Sb_{0.10}O_{3-\delta}$	15.37	28.34
$SrCo_{0.85}Sb_{0.15}O_{3-\delta}$	14.88	29.29

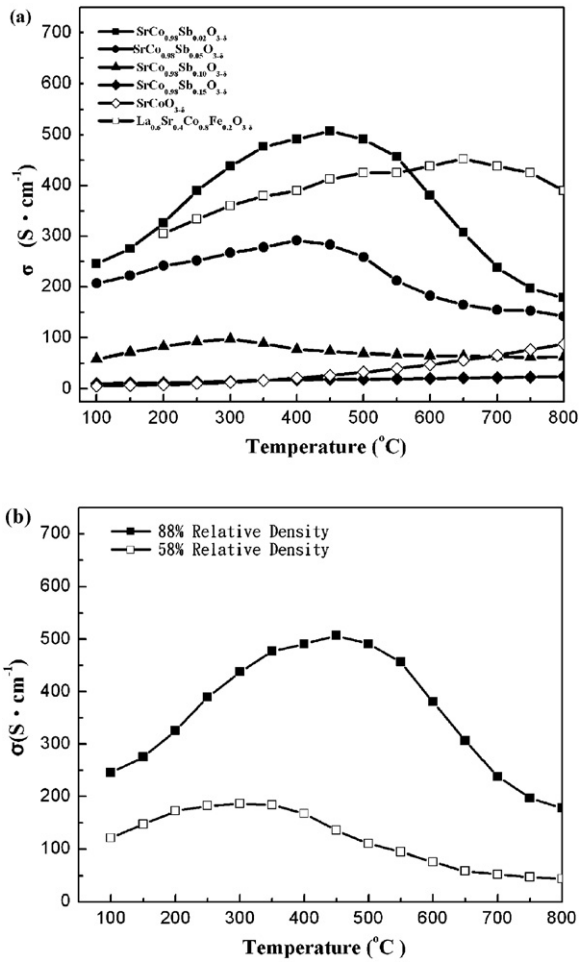

Fig. 4. Electrical conductivities of (a) $SrCo_{0.98}Sb_{0.02}O_{3-\delta}$, $SrCo_{0.95}Sb_{0.05}O_{3-\delta}$, $SrCo_{0.9}Sb_{0.1}O_{3-\delta}$, and $SrCo_{0.85}Sb_{0.15}O_{3-\delta}$ ceramics sintered at 1175 °C for 24 h and (b) $SrCo_{0.98}Sb_{0.02}O_{3-\delta}$ ceramics with relative densities of 88% and 58%.

$SrCo_{0.85}Sb_{0.15}O_{3-\delta}$ ceramics sintered at 1175 °C for 24 h. The conductivities of the perovskite cathodes increased with the temperature, reached their peaks at temperatures ranging approximately from 300 to 600 °C and started to drop with further rise in the temperature. The peaks probably corresponded to the temperatures at which oxygen exchange of the materials started to create an increasing number of vacancies to compete with hole carriers [24]. This was in fact to be expected since $2CO_{CO}^{\bullet} + o_O^x \Leftrightarrow 2CO_{CO}^x + V_O^{\bullet\bullet} + 1/2\ O_2(g)$ [12]. At lower temperatures ($T < 300$ K), the conductivity shows a thermally activated behavior and rose with the temperature due to the increased mobility of the electronic charge carriers $Co_{Co}^{\bullet}$ which represent the holes localized on B sites. At higher temperatures, on the other hand, the electronic conductivity is reduced by the decrease in the number of p-type charge carriers due to the progressive formation of oxygen vacancies at the expense of $Co_{Co}^{\bullet}$ [28,29]. This appears to agree with the temperature-induced change in dimension as shown in Fig. 3. Compared to pure $SrCoO_{3-\delta}$, introducing antimony ions in the position of cobalt ions significantly props up the electrical conductivity, mainly due to the antimony ions' stabilizing the 3D framework of the corner-sharing CoO_6 octahedra with the

open Co–O–Co angle to facilitate the overlapping of Co(3d)–O(2p) orbital. A maximum electrical conductivity of 507 S/cm was obtained for the $SrCo_{0.98}Sb_{0.02}O_{3-\delta}$ ceramic at 450 °C. After hitting the highest point, however, the electrical conductivity started to decline considerably with further increase in the content of the antimony ions. A similar behavior was observed by Aguadero et al. [15], who reported that the highest conductivity value, present in the $x = 0.05$ sample, read 505 S/cm at 400 °C [15]. For the MIEC perovskites, transport of oxygen ions (ionic conduction) proceeded by the hopping of the oxygen vacancies while transport of electrons (electronic conduction) continued along the B^{n+}–O^{2}–$B^{(n-1)+}$ network due to the overlapping between the transition metal 3d orbital and the oxygen 2p orbital. With increased doping of antimony ions, the nonconducting Sb–O bonds increased to hinder the electronic transport [12,15], leading to lower electrical conductivity. In consideration of the densification effect as shown in Fig. 4(b), the differences in the electrical conductivity of the $SrCo_{1-y}Sb_yO_{3-\delta}$ ceramics are expected to expand with respect to the content of the doped antimony ions. The $SrCo_{0.98}Sb_{0.02}O_{3-\delta}$ ceramics with relative densities of 88% and 58% reported maximum electrical conductivities of 507 S/cm at 450 °C and 186 S/cm at 300 °C respectively. Higher densification helps improve electrical conductivity and increase the mobility of the electronic charge carriers, subsequently resulting in a higher maximum electrical temperature.

To identify the compatible electrolyte materials for the $SrCo_{1-y}Sb_yO_{3-\delta}$ cathode, electrolytes including YSZ, SDC, and LSGM were mixed with the $SrCo_{1-y}Sb_yO_{3-\delta}$ cathode at a weight ratio of 1:1, heated up to 1100 °C for 2 h, and then phase examined by XRD analysis. The results indicated that the mixture of YSZ and $SrCo_{1-y}Sb_yO_{3-\delta}$ led to the formation of second phase $SrZrO_3$ while SDC and LSGM reported no chemical reaction with $SrCo_{1-y}Sb_yO_{3-\delta}$. Accordingly, single cells with the $SrCo_{1-y}Sb_yO_{3-\delta}$ cathode and SDC electrolyte were prepared in this study for electrochemical measurements. Two types of cathodes, including a pure $SrCo_{1-y}Sb_yO_{3-\delta}$ cathode and a composite cathode of 60 wt% $SrCo_{1-y}Sb_yO_{3-\delta}$ and 40 wt% SDC, were screen printed on the anode-supported substrate with the fired thickness set at ≈50 μm. The anode supported substrate incorporates an anode electrode with a total thickness of nearly 0.5 mm and a SDC electrolyte approximately 13 μm in thickness. The anode electrode is composed of three layers, including a NiO current collector layer (thickness ≈20 μm) plus a 60 wt% NiO/40 wt% SDC (thicknesses ≈460 μm) and a 50 wt% NiO/50 wt% SDC (thickness ≈6 μm) functional composite layers. The SDC electrolyte is dense and crack-free with some scattering closed pores.

Fig. 5(a) and (b) present the Nyquist plots of the electrochemical impedance spectra of the anode supported single cells with respectively a $SrCo_{0.98}Sb_{0.02}O_{3-\delta}$ cathode and a $SrCo_{0.98}Sb_{0.02}O_{3-\delta}$-SDC composite cathode, measured at different temperatures. The highest frequency intercept of the impedance spectra gives the total ohmic resistance of the cell (R_0), including the resistive contributions of the electrolyte, the two electrodes, the current collectors, and the lead wires, as

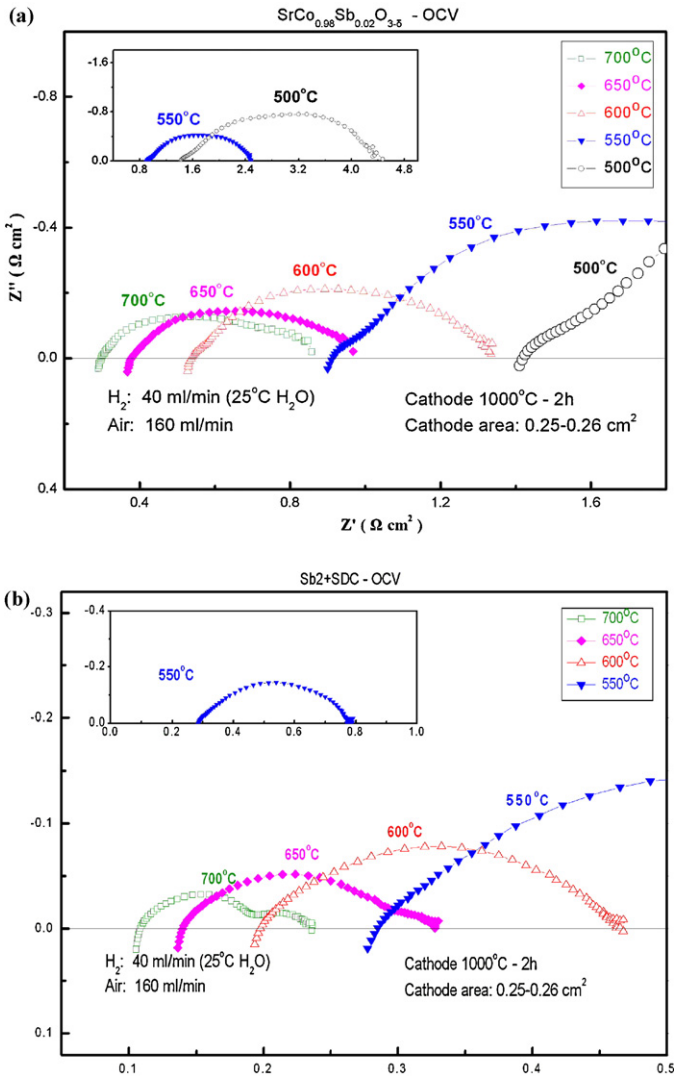

Fig. 5. Impedance spectra of anode supported single cells incorporating (a) a $SrCo_{0.98}Sb_{0.02}O_{3-\delta}$ cathode, and (b) a $SrCo_{0.98}Sb_{0.02}O_{3-\delta}$–SDC composite cathode measured at different temperatures.

reported in the literature [21,30,31]. The lowest frequency intercept corresponds to the overall resistance of the cell, and the distance between the two intercepts gives the total interfacial polarization resistance (R_P) [9]. The polarization loss resulting from the anode side is generally small enough to be disregarded as compared to its counterpart from the cathode side [25,32,33]. The R_0 values of the single cell with the pure $SrCo_{0.98}Sb_{0.02}O_{3-\delta}$ cathode at 700 °C and 600 °C read respectively 0.298 Ω cm^2 and 0.538 Ω cm^2 while the R_P values emerged to be 0.560 Ω cm^2 and 0.793 Ω cm^2. The single cell with the $SrCo_{0.98}Sb_{0.02}O_{3-\delta}$-SDC composite cathode appeared to reduce the impedances, in which the R_0 values at 700 °C and 600 °C read 0.109 Ω cm^2 and 0.198 Ω cm^2 and the R_P values reported 0.127 Ω cm^2 and 0.270 Ω cm^2. Apparently, both ohmic and polarization resistances increase with decreasing operating temperature. The low R_0 and R_P values described above reveal the potential of the $SrCo_{0.98}Sb_{0.02}O_{3-\delta}$ ceramic to serve as a cathode for IT-SOFCs, a feature further verified by the results of the cell performance analysis shown in Fig. 6.

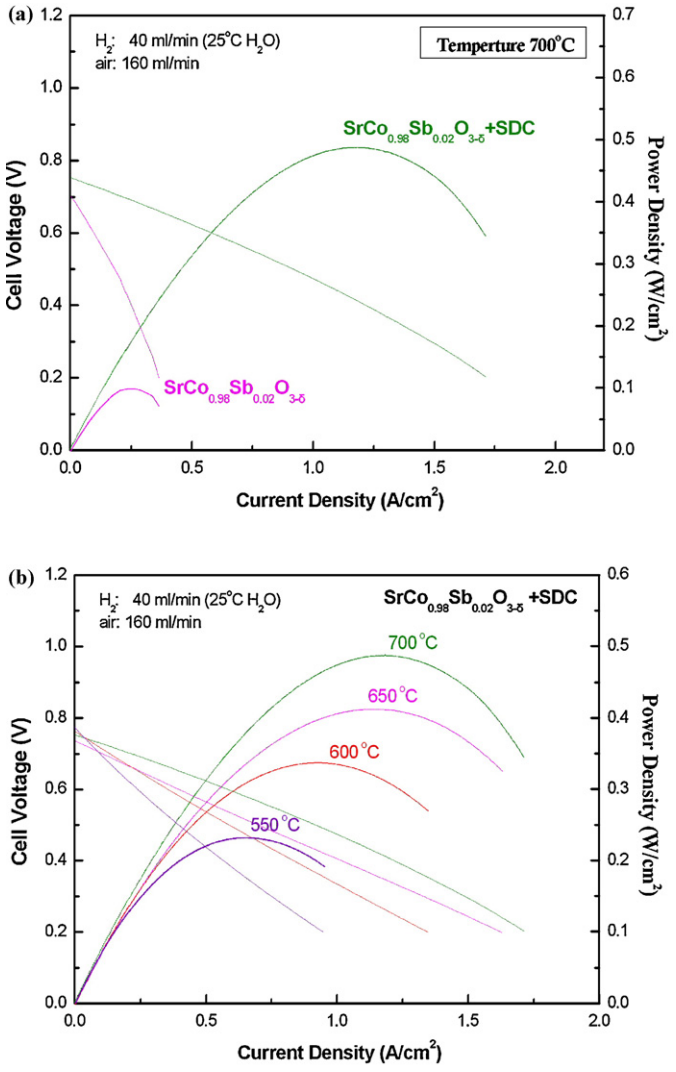

Fig. 6. *I–V* curves and the corresponding power densities of the anode supported single cells showing (a) a comparison of $SrCo_{0.98}Sb_{0.02}O_{3-\delta}$ and $SrCo_{0.98}Sb_{0.02}O_{3-\delta}$–SDC composite cathodes measured at 700 °C, and containing (b) a $SrCo_{0.98}Sb_{0.02}O_{3-\delta}$–SDC composite cathode measured at different temperatures.

Fig. 6(a) compares the cell performances of the anode supported SOFC single cells, the pure $SrCo_{0.98}Sb_{0.02}O_{3-\delta}$ cathode, and the $SrCo_{0.98}Sb_{0.02}O_{3-\delta}$-SDC composite cathodes measured at 700 °C. It should be noted that the pure $SrCo_{0.98}Sb_{0.02}O_{3-\delta}$ cathode peeled off from the single cell after electrochemical measurement due to the substantial difference in terms of thermal expansion between the cathode and the electrolyte. The single cell with the $SrCo_{0.98}Sb_{0.02}O_{3-\delta}$-SDC composite cathode, on the other hand, retained good structural integrity after measurement. With no microstructure optimization, the single cells with the pure $SrCo_{0.98}Sb_{0.02}O_{3-\delta}$ cathode and the $SrCo_{0.98}Sb_{0.02}O_{3-\delta}$–SDC composite cathode measured at 700 °C reported maximum power densities of 0.100 W/cm^2 and 0.487 W/cm^2 respectively, coincident with the impedance spectra illustrated in Fig. 5. As indicated by Fig. 6(b) that shows the cell performance of the single cell with the $SrCo_{0.98}Sb_{0.02}O_{3-\delta}$–SDC composite cathode as a function of the operating temperature, the OCVs of the single cells ranged from 0.75 V to 0.8 V, all lower than the expected theoretical values because of the mixed ionic and electronic conduction of the SDC electrolyte in the reducing atmosphere [5]. The OCV of the cell declined slightly as the temperature increased, except for the value at 600 °C which was lower than that at 700 °C possibly due to gas leakage during measurement. Maximum power densities (MPD) dropped with decreasing operating temperature from 0.487 to 0.232 W/cm^2 as the temperature was reduced from 700 °C to 500 °C due to the increase of the R_0 and R_P of the single cells. Apparently, the $SrCo_{1-y}Sb_yO_{3-\delta}$ ceramic is a potential cathode for IT-SOFC applications.

4. Conclusions

As indicated by the study, doping of antimony ions not only stabilized the Pm3m phase of the $SrCo_{1-y}Sb_yO_{3-\delta}$ ceramics but also enhanced densification and retarded grain growth. A maximum electrical conductivity of 507 S/cm was obtained for the $SrCo_{0.98}Sb_{0.02}O_{3-\delta}$ ceramic at 450 °C. The single cell with the $SrCo_{0.98}Sb_{0.02}O_{3-\delta}$–SDC composite cathode appeared to reduce the impedances, in which the R_0 and R_P at 700 °C were measured to be 0.109 Ω cm^2 and 0.127 Ω cm^2 respectively, as compared to the cell with the pure $SrCo_{0.98}Sb_{0.02}O_{3-\delta}$ cathode. The maximum power densities of the single cells with the $SrCo_{0.98}Sb_{0.02}O_3$–SDC composite cathodes measured at 700 °C read 0.487 W/cm^2.

References

[1] M.D. Mata, X. Liub, Z. Zhu, B. Zhu, Development of cathodes for methanol and ethanol fuelled low temperature (300–600 °C) solid oxide fuel cells, International Journal of Hydrogen Energy 32 (2007) 796–801.
[2] T.L. Wen, D. Wang, M. Chen, H. Tu, Z. Lu, Z.R. Zhang, H. Nie, Material research for planar SOFC stack, Solid State Ionics 148 (2002) 513–519.
[3] E. Ivers-Tiffée, A. Weber, D. Herbstritt, Materials and technologies for SOFC components, Journal of the European Ceramic Society 21 (2001) 1805–1811.
[4] M. Zhang, M. Yang, Z. Hou, Y. Dong, M. Cheng, A bi-layered composite cathode of $La_{0.8}Sr_{0.2}MnO_3$-YSZ and $La_{0.8}Sr_{0.2}MnO_3$-$La_{0.4}Ce_{0.6}O_{1.8}$ for IT-SOFCs, Electrochimica Acta 53 (2008) 4998–5006.
[5] J.W. Fergus, Electrolytes for solid oxide fuel cells, Journal of Power Sources 162 (2006) 30–40.
[6] S.B. Adler, Factors governing oxygen reduction in solid oxide fuel cell cathodes, Chemical Reviews 104 (2004) 4791–4843.
[7] J.M. Ralph, A.C. Schoeler, M. Krumpelt, Materials for lower temperature solid oxide fuel cells, Journal of Materials Science 36 (2001) 1161–1172.
[8] J.M. Ralph, C. Rossignol, R. Kumar, Cathode materials for reduced-temperature SOFCs, Journal of Electrochemical Society 150 (2003) A1518–A1522.
[9] W.G. Guo, J. Liu, C. Jin, H. Gao, Y. Zhang, Electrochemical evaluation of $La_{0.6}Sr_{0.4}Co_{0.2}Fe_{0.8}O_{3-\delta}$-$La_{0.9}Sr_{0.1}Ga_{0.8}Mg_{0.2}O_{3-\delta}$ Composite Cathodes for $La_{0.9}Sr_{0.1}Ga_{0.8}Mg_{0.2}O_{3-\delta}$ electrolyte SOFCs, Journal of Alloys and Compounds 473 (2009) 43–47.
[10] M. Prestat, J.F. Koenig, L.J. Gauckler, Oxygen reduction at thin dense $La_{0.52}Sr_{0.48}Co_{0.18}Fe_{0.82}O_{3-\delta}$ electrodes, Journal of Electroceramics 18 (2007) 87–101.
[11] X. Ding, X. Kong, J. Jiang, C. Cui, L. Guo, Electrical performance of $La_{0.7}Sr_{0.3}Cu_{3-\delta}$-$Sm_{0.2}Ce_{0.8}O_{2-\delta}$ functional graded composite cathode for intermediate temperature solid state fuel cells, International Journal of Hydrogen Energy 35 (2010) 1742–1748.
[12] F. Wang, Q. Zhou, T. He, G. Li, H. Ding, Novel $SrCo_{1-y}Nb_yO_{3-\delta}$ cathodes for intermediate-temperature solid oxide fuel cells, Journal of Power Sources 195 (2010) 3772–3778.

[13] W. Zhou, W. Jin, Z. Zhu, Z. Shao, Structural, electrical and electrochemical characterizations of $SrNb_{0.1}Co_{0.9}O_{3-\delta}$ as a cathode of solid oxide fuel cells operating below 600 °C, International Journal of Hydrogen Energy 35 (2010) 1356–1366.

[14] P. Zeng, R. Ran, Z. Chen, W. Zhou, H. Gu, Z. Shao, S. Liu, Efficient stabilization of cubic Perovskite $SrCoO_{3-\delta}$ by B-site low concentration scandium doping combined with sol–gel synthesis, Journal of Alloys and Compounds 455 (2008) 465–470.

[15] A. Aguadero, D. Perez-Coll, C. de la Calle, J.A. Alonso, M.J. Escudero, L. Daza, $SrCo_{1-x}Sb_xO_{3-\delta}$ Perovskite oxides as cathode materials in solid oxide fuel cells, Journal of Power Sources 192 (2009) 132–137.

[16] J.H. Kim, S.W. Baek, C. Lee, K. Park, J. Bae, Performance analysis of cobalt-based cathode materials for solid oxide fuel cells, Solid State Ionics 179 (2009) 132–137.

[17] T. Nagai, W. Ito, T. Sakon, Relationship between cation substitution and stability of Perovskite structure in $SrCoO_{3-\delta}$-based mixed conductors, Solid State Ionics 177 (2007) 3433–3444.

[18] A.L. Shaula, V.V. Kharton, F.M.B. Marques, A.V. Kovalevsky, A.P. Viskup, E.N. Naumovich, Phase interaction and oxygen transport in oxide composite materials, British Ceramic Transactions 103 (2004) 211–218.

[19] S.F. Wang, Y.R. Wang, C.T. Yeh, Y.F. Hsu, S.D. Chyou, W.T. Lee, Effects of Bi-layer LSCF-based cathodes on characteristics of intermediate temperature SOFCs, Journal of Power Sources 196 (2011) 977–987.

[20] X. Ding, C. Cui, L. Guo, Thermal expansion and electrical performance of $L_{0.7}Sr_{0.3}CuO_{3-\delta}$-$Sm_{0.2}Ce_{0.8}O_{2-\delta}$ composite cathode for IT-SOFC, Journal of Alloys and Compounds 481 (2008) 845–850.

[21] E.P. Murray, S.A. Barnett, (La,Sr)MnO_3-(Ce,Gd)O_{2-x} composite cathodes for solid oxide fuel cells, Solid State Ionics 143 (2001) 265–273.

[22] X. Xu, Z. Jiang, X. Fan, C. Xia, LSM-SDC Electrodes fabricated with an ion-impregnating process for SOFCs with doped ceria electrolytes, Solid State Ionics 177 (2006) 2113–2117.

[23] J. Chen, F. Liang, B. Chi, J. Pu, S.P. Jiang, L. Jian, Palladium and ceria infiltrated $La_{0.8}Sr_{0.2}Co_{0.5}Fe_{0.5}O_{3-\delta}$ cathodes of solid oxide fuel cells, Journal of Power Sources 194 (2009) 275–280.

[24] R.N. Basu, A. Das Sharma, A. Dutta, J. Mukhopadhyay, Processing of high-performance anode-supported planar solid oxide fuel cell, International Journal of Hydrogen Energy 33 (2008) 5748–5754.

[25] C. Xia, M. Liu, Novel cathodes for low temperature solid oxide fuel cell, Advanced Materials 14 (2002) 521–523.

[26] X. Xu, C. Xia, G. Xiao, D. Peng, Fabrication and performance of functionally graded cathodes for IT-SOFCs based on doped ceria electrolytes, Solid State Ionics 176 (2005) 1513–1520.

[27] T.L. Reitz, H. Xiao, Characterization of electrolyte-electrode interlayers in thin film solid oxide fuel cell, Journal of Power Sources 161 (2006) 437–443.

[28] P. Ried, P. Holtappels, A. Wichser, A. Ulrich, T. Graule, Synthesis and characterization of $Ba_{0.5}Sr_{0.5}Co_{0.8}Fe_{0.2}O_{3-\delta}$ and $La_{0.6}Sr_{0.4}Co_{0.2}Fe_{0.8}O_{3-\delta}$, Journal of Electrochemical Society 155 (2008) B1029–B1035.

[29] J. Van Herle, R. Ihringer, R. Vasquez Cavieres, L. Constantin, O. Bucheli, Anode supported solid oxide fuel cells with screen-printed cathodes, Journal of the European Ceramic Society 21 (2001) 1855–1859.

[30] E.P. Murray, T. Tsai, S.A. Barnett, Oxygen transfer processes in (La,Sr)MnO_3/Y_2O_3-stabilized ZrO_2 cathodes: an Impedance Spectroscopy Study, Solid State Ionics 110 (1998) 235–247.

[31] Fuel Cell Handbook, 7th edition, EG&G Technical Services, Inc, USDOE, 2004, pp. 7-18.

[32] Q.A. Huang, R. Hui, B. Wang, J. Zhang, A review of AC impedance modeling and validation in SOFC diagnosis, Electrochimica Acta 52 (2007) 8144–8164.

[33] C. Fu, S.H. Chan, Q. Liu, X. Ge, G. Pasciak, Fabrication and evaluation of Ni-GDC composite anode prepared by aqueous-based tape casting method for low-temperature solid oxide fuel cell, International Journal of Hydrogen Energy 35 (2010) 301–307.